frontiers | Frontiers in Physics

TYPE Original Research
PUBLISHED 13 September 2023
DOI 10.3389/fphy.2023.1257937

Check for updates

OPEN ACCESS

EDITED BY
Airton Deppman,
University of São Paulo, Brazil

REVIEWED BY
Ying Yuan,
Guangxi University of Chinese Medicine, China
Waqas Muhammad,
Hubei University of Automotive Technology, China
Junsheng Li,
Shanxi Normal University, China

*CORRESPONDENCE
Bao-Chun Li,
s6109@sxu.edu.cn

RECEIVED 13 July 2023
ACCEPTED 24 August 2023
PUBLISHED 13 September 2023

CITATION
Geng Y-F and Li B-C (2023), Properties of the particle distribution in Pb−Pb collisions at $\sqrt{s_{NN}}$ = 5.02 TeV and $\sqrt{s_{NN}}$ = 2.76 TeV.
Front. Phys. 11:1257937.
doi: 10.3389/fphy.2023.1257937

Properties of the particle distribution in Pb−Pb collisions at $\sqrt{s_{NN}}$ = 5.02 TeV and $\sqrt{s_{NN}}$ = 2.76 TeV

Yan-Feng Geng[1,2] and Bao-Chun Li[1,2]*

[1]College of Physics and Electronics Engineering, Shanxi University, Taiyuan, Shanxi, China, [2]Collaborative Innovation Center of Extreme Optics, Shanxi University, Taiyuan, Shanxi, China

Properties of the particle distribution in high energy heavy-ion collisions are important for understanding the particle production. In Tsallis statistics with a multisource production, we study the transverse momentum spectra of D^0, D^+, D^{*+}, D_s^+, J/ψ in Pb−Pb collisions at $\sqrt{s_{NN}}$ = 5.02 TeV and charged particles in Pb−Pb collisions at $\sqrt{s_{NN}}$ = 2.76 TeV. A good agreement can be observed between the results obtained in the model and the experimental results of ALICE and CMS collaboration. The nuclear modification factor R_{AA} is reproduced. Properties reflected in the multiparticle system are discussed by the parameters provided in the improved model. It is found that the temperature T and the t_{ft}/τ increase with the centrality for the same particle due to the excitation degree of the multiparticle system. The non-equilibrium degree at $\sqrt{s_{NN}}$ = 5.02 TeV is larger than that at $\sqrt{s_{NN}}$ = 2.76 TeV. It shows that the system at the larger collision energy deviates farther from the equilibrium state.

KEYWORDS

Tsallis statistics, multisource production, transverse momentum spectra, nuclear modification factor, high-energy heavy-ion collisions

1 Introduction

The transverse momentum p_T spectra of particles produced in heavy-ion collisions at high energies are important observables and can provide valuable information about the collision system. They are often used to discuss the particle-production properties of the collision system. A large amount of p_T experimental data in pp collisions at different energies and nucleus–nucleus (AA) collisions for different centralities at different energies has been measured using the Relativistic Heavy Ion Collider (RHIC) [1, 2] and the Large Hadron Collider (LHC) [3, 4]. The initial distribution of the high-energy particles can be parameterized by the Tsallis distribution [5, 6], which extracted the Tsallis temperature T and a nonextensivity parameter q. The nonextensivity parameter was used to describe the degree of a non-equilibrium of the system. A thermodynamically consistent form of the Tsallis distribution was taken to fit the transverse momentum spectra. As a new matter, quark–gluon plasma (QGP) is a thermalized system composed of strongly coupled quarks and gluons in a finite area. The high-energy particles finally lose energy when they interact with the QGP medium, which is formed due to collision of heavy ions with each other. The distribution modification due to energy loss reveals the characteristics of the matter produced in collisions. The effects of the energy loss and the dynamics of hadronization can be studied using the nuclear modification factor R_{AA}, which compares the transverse momentum differential production yields in nucleus–nucleus collisions ($d^2N_{AA}/dydp_T$) with the transverse momentum differential production yields in inelastic proton–proton collisions ($d^2\sigma_{pp}/dydp_T$).

Particle distribution is a significant value observed in the LHC experiment. Many phenomenological models were proposed to discuss the abundant experimental data. However, it is very difficult to uniformly describe the whole properties of particle distribution and to analyze the whole process of matter evolution in relativistic heavy-ion collisions by using only one method. In recent years, some different methods were combined with each other in order to figure out the multiparticle production in heavy-ion collisions at high energies. Recently, different statistic-based models were proposed to understand the transverse momentum p_T distribution of final-state particles in high-energy collisions, such as the statistical thermal model [7, 8], the statistical hadronization model [9], Tsallis statistics [10], the wounded quark model [11], Boltzmann statistics [12], the multisource thermal model [13], Rayleigh distribution [14], and Erlang distribution [15]. In particular, Tsallis statistics has successfully described the experimental p_T distribution, longitudinal momentum fraction distribution, and the rapidity distribution of hadrons produced in high-energy collisions [16, 17]. It was widely applied by STAR [18] and PHENIX [19] collaborations at RHIC and by ALICE [20–25], ATLAS [26], and CMS [27, 28] collaborations at LHC.

Heavy-flavor quarks are mostly produced in the initial stage of collisions in hard scattering processes between nucleus partons. Heavy-flavor quarks can undergo the whole evolution process of QGP created in ultra-relativistic heavy-ion collisions. Therefore, heavy-flavor mesons carry the substantial information of the hot-dense QCD medium and hadron production and are recognized as important probes of the QGP. It is crucial to study the interaction between heavy-flavor quarks and the strongly interacting medium by the differential production yield, the nuclear modification factor, and the anisotropic collective flow of heavy-flavor mesons. Thermodynamic properties were obtained via the comparison of theoretical models with transverse momentum spectra p_{T} of heavy-flavor mesons measured in collisions. The nuclear modification factor R_{AA} is a key observable, allowing us to discuss the mechanisms of the particle production in proton–proton collisions and heavy-ion collisions at high energies and understand the effects of energy loss and the dynamics of the heavy-quark hadronization. In the investigation of the transverse momentum p_{T} spectra of heavy-flavor mesons, some parameters required in the model calculation of the nuclear modification factor R_{AA} may be extracted synchronously.

The transverse momentum spectra of final-state particles can give the significant information of the produced matter in high-energy collisions. In our previous work [29], the temperature parameters of particle-emission sources were determined qualitatively in the geometrical manner of the multisource thermal model, and thermodynamic properties of these emission sources were determined from the central axis to the side-surface of the source cylinder. In this paper, we will investigate the transverse momentum distributions of prompt D^0, D^+, D^{*+}, and D_s^+ mesons for different centralities and prompt J/ψ in Pb–Pb collisions at $\sqrt{s_{NN}} = 5.02$ TeV. Furthermore, the transverse momentum p_T distribution of charged particles for different centralities in Pb–Pb collisions at $\sqrt{s_{NN}} = 2.76$ TeV is compared with the transverse momentum up to 100 GeV/c . Based on the analysis, the nuclear modification factors will be reproduced. In most of our previous works [29, 30], the multisource thermal model was used mainly to discuss the transverse momentum spectra in different collisions at high energies. In this work, we will combine a new method with the multisource production to investigate the distribution of particles produced in Pb–Pb collisions at $\sqrt{s_{NN}}$ = 5.02 TeV and $\sqrt{s_{NN}}$ = 2.76 TeV. This work is a new attempt and will help us understand the properties of particle distribution in high-energy heavy-ion collisions from more different perspectives.

2 Particle distribution in Tsallis statistics

In the multisource thermal model [29], the projectile and target cylinders were supposed to be formed in nucleus–nucleus collisions at high energy. In the rapidity space, the projectile cylinder and the target cylinder lie in the rapidity range [-Y, Y]. The final-state particles are produced from different emission sources in the cylinders. Final-state particles emit anisotropically from these emission sources in different longitudinal locations. On the other hand, the projectile and target cylinder are thought to be composed of a series of emission sources with different rapidity shifts. The model is commonly known as a multisource thermal model. The simple model can only describe transverse momentum spectra of particles and can only identify the qualitative temperature parameters of emission sources by transverse momentum spectra. The limitation of the model is very difficult to avoid. In this work, the multisource production will be considered in Tsallis statistics, which is a thermodynamic formalism of describing the fractal structure of Yang–Mills fields [31, 32]. In addition, the relaxation time approximation of the collision term in the Boltzmann transport equation will be introduced into the model in order to describe the p_T distribution and the nuclear modification factor R_{AA}. Using the improved model, the particle distribution in experiments is explained in the new formalism. The different interpretations complement one another and allow us to understand the particle production from various perspectives. In the improved model, the thermodynamic properties of the multiparticle system are discussed further compared to our previous works.

In the calculation, we consider a thermodynamically consistent form of the Tsallis distribution, which was described in detail in Refs [5, 33]. From the Tsallis distribution, the correlative thermodynamic quantities can be extracted. According to Tsallis statistics, the particle number is given by

$$N = gV \int \frac{d^3p}{(2\pi)^3}\left[1 + (q-1)\frac{E-\mu}{T}\right]^{-\frac{q}{q-1}}, \tag{1}$$

where g, V, p, E, and μ are the degeneracy factor, volume, particle momentum, energy, and chemical potential, respectively. The parameter T is a Tsallis temperature, and q

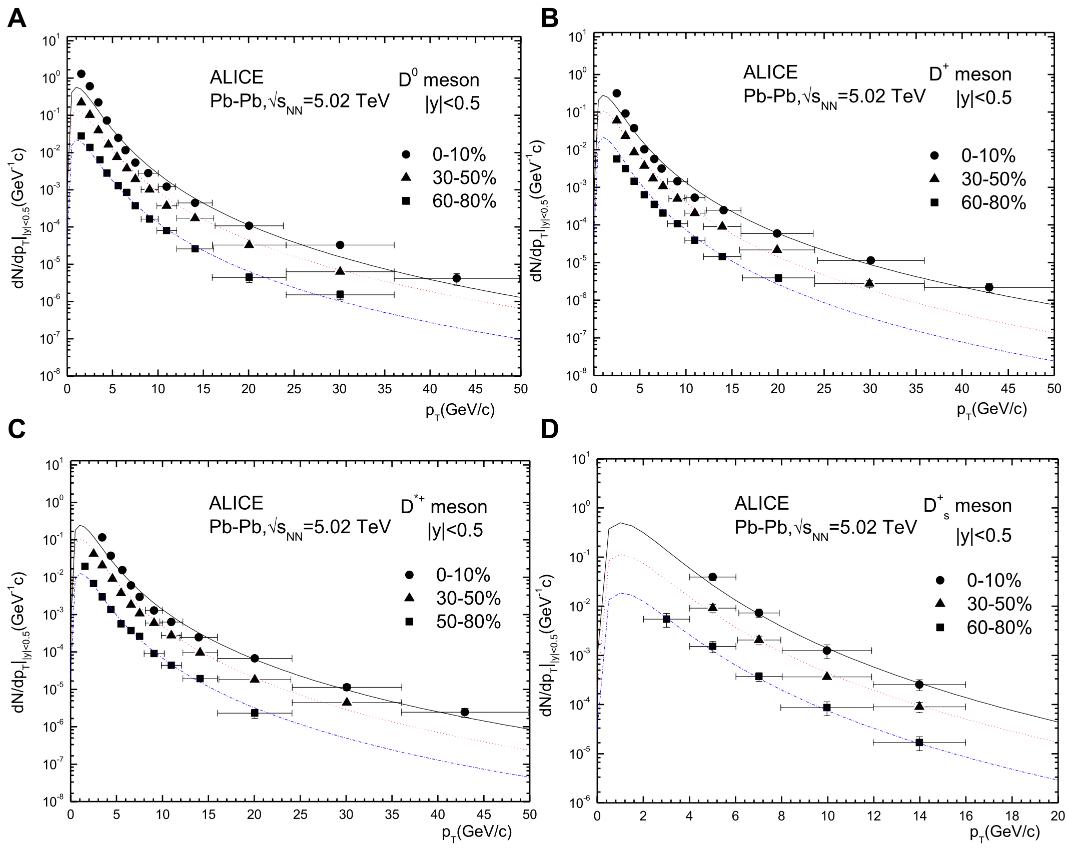

FIGURE 1
Transverse momentum distributions of prompt D^0 **(A)**, D^+ **(B)**, D^{*+} **(C)**, and D_s^+ **(D)** mesons in the 0%–10%, 30%–50%, and 60%–80% centrality classes in Pb–Pb collisions at $\sqrt{s_{NN}}$ = 5.02 TeV. Statistical uncertainties (bars) are shown. Symbols represent the experimental results obtained from ALICE collaboration [32]. The model results are represented by the curves.

is a nonextensivity parameter. The corresponding momentum distribution is given by

$$\frac{d^3N}{d^3p} = \frac{gV}{(2\pi)^3}\left[1 + (q-1)\frac{E-\mu}{T}\right]^{-\frac{q}{q-1}}. \tag{2}$$

When the nonextensivity parameter q tends to 1, the distribution function is the Boltzmann distribution, given by

$$\lim_{q \longrightarrow 1} \frac{d^3N}{d^3p} = \frac{gV}{(2\pi)^3}\exp\left(-\frac{E-\mu}{T}\right). \tag{3}$$

Considering the multisource emission [29, 30], the transverse momentum distribution of initial-state particles can be written as

$$f_{it} = \int_{-Y}^{Y} \frac{gV}{(2\pi)^2} p_T m_T \left[1 + (q-1)\frac{m_T}{T}\right]^{-\frac{q}{q-1}} dy. \tag{4}$$

In the calculation, Eq. 4 is regarded as an initial distribution of the Boltzmann transport equation. By the relaxation time approximation of the collision term, the Boltzmann transport equation is solved in order to obtain a distribution of final-state particles.

The nuclear modification factor R_{AA} is

$$R_{AA} = \frac{f_{ft}}{f_{it}}, \tag{5}$$

where f_{ft} is a distribution function of final-state particles.

An evolution of the particle distribution $f(\vec{x}, \vec{p}, t)$ is given by the Boltzmann transport equation:

$$\frac{df(\vec{x}, \vec{p}, t)}{dt} = \frac{\partial f}{\partial t} + \vec{v} \cdot \vec{\nabla}_x f + \vec{F} \cdot \vec{\nabla}_p f, \tag{6}$$

where $\vec{v}$ is a velocity and $\vec{F}$ is an external force. In order to account for the collision, the equation is written as

$$\frac{df(\vec{x}, \vec{p}, t)}{dt} = \left(\frac{\partial f}{\partial t}\right)_{coll}. \tag{7}$$

By considering the relaxation time approximation, the collision term $(\frac{\partial f}{\partial t})_{coll}$ is given by

$$\left(\frac{\partial f}{\partial t}\right)_{coll} = -\frac{f - f_{et}}{\tau}, \tag{8}$$

where τ is a relaxation time. The function f_{et} is a distribution function of particles in the Boltzmann local equilibrium state:

$$f_{et} = \frac{gV}{(2\pi)^2} p_T m_T e^{-\frac{m_T}{T_{et}}}, \tag{9}$$

where T_{et} is the equilibrium temperature. Considering a homogeneous distribution and $\vec{F} = 0$ in Eq. 6, the distribution of final-state particles produced in collisions is

$$f_{ft} = f_{et} + (f_{it} - f_{et}) e^{-\frac{t_{ft}}{\tau}}. \tag{10}$$

By using Eq. 5, the nuclear modification factor [6] is given by

$$R_{AA} = \frac{f_{ft}}{f_{it}} = \frac{f_{et}}{f_{it}} + \left(1 - \frac{f_{et}}{f_{it}}\right) e^{\frac{-t_{ft}}{\tau}}. \tag{11}$$

3 Comparison and discussion

Figure 1 shows the transverse momentum spectra of prompt D^0, D^+, D^{*+}, and D_s^+ mesons for 0%–10%, 30%–50%, and 60%–80% centrality classes in Pb–Pb collisions at $\sqrt{s_{NN}} = 5.02$ TeV. Figures 1A–D show D^0, D^+, D^{*+}, and D_s^+, respectively. The scattered symbols indicate the experimental data obtained from ALICE collaboration [34]. The lines represent the model results, which are in agreement with the experimental results. For low-p_T data, the model results are inconsistent with experimental data in central collisions. However, the major trend of the data change is similar. The parameter values taken in the calculation are listed in Table 1. For the same meson, the temperature T and t_{ft}/τ increase with the centrality. The reaction system is subjected to high excitation because the number of participating nucleons increases with centrality. It is shown that the reaction system in central collisions requires less time to reach the local equilibrium due to the initial distribution. Using the parameters and Eq. 11, the nuclear modification factor R_{AA} of these mesons for different centralities is obtained.

TABLE 1 Fitted values of q, T, and t_{ft}/τ shown in Figure 1 and Figure 3.

Particle	Centrality	q	T	t_{ft}/τ
D^0	0%–10%	1.163	0.156	1.502
	30%–50%	1.170	0.150	0.900
	60%–80%	1.173	0.137	0.456
D^+	0%–10%	1.164	0.155	1.484
	30%–50%	1.169	0.149	0.896
	60%–80%	1.172	0.140	0.435
D^{*+}	0%–10%	1.164	0.151	1.510
	30%–50%	1.168	0.146	0.882
	60%–80%	1.171	0.140	0.405
D_s^+	0%–10%	1.152	0.151	1.320
	30%–50%	1.157	0.148	0.505
	60%–80%	1.160	0.146	0.201
J/Ψ	0%–100%	1.150	0.158	1.060

Figure 2 shows the nuclear modification factor R_{AA} of prompt D^0, D^+, D^{*+}, and D_s^+ mesons in the 0%–10%, 30%–50%, and 60%–80% centrality classes in Pb–Pb collisions at $\sqrt{s_{NN}} = 5.02$ TeV. The scattered symbols represent the experimental data obtained from ALICE collaboration [34]. The lines represent the model results. Compared with Figure 1, the model results of Figure 2 are approximately consistent with the experimental data. The model values are not close to the low-p_T experimental data due to other processes, such as regeneration and shadowing.

Figure 3 shows the transverse momentum spectra of the prompt J/ψ meson in Pb–Pb collisions at $\sqrt{s_{NN}} = 5.02$ TeV. The scattered symbols indicate the experimental data obtained from CMS collaboration [35]. The maximum of the transverse momentum is 50 GeV/c. The lines represent the model results, which are in agreement with the experimental results. The parameter values are listed in Table 1. The nuclear modification factor R_{AA} of J/ψ is shown in Figure 4.

To further test the capacity of the model, we analyze other particles at a higher energy. Figure 5 shows the transverse momentum spectra of charged particles for 0%–5%, 5%–10%, 10%–30%, 30%–50%, 50%–70%, and 70%–90% centrality classes in Pb–Pb collisions at $\sqrt{s_{NN}} = 2.76$ TeV. The scattered symbols indicate the experimental data obtained from CMS collaboration [36]. The lines represent the model results, which are in agreement with the experimental results. The parameter values and χ^2/NDF (number of degrees of freedom) are listed in Table 2. The temperature T and t_{ft}/τ increase with the centrality. Overall, the values of parameters T, q, and t_{ft}/τ are smaller than those at $\sqrt{s_{NN}} = 5.02$ TeV. In the calculation, charged particles $\pi^{\pm}$, $K^{\pm}$, p, and $\bar{p}$ are considered [37].

By analyzing the results, it is revealed that the improved model can explain the transverse momentum p_T spectra of particles produced in collisions and reproduce R_{AA} approximately. Furthermore, thermodynamic properties of the multiparticle system are discussed.

4 Conclusion

In our previous works [29, 30], the multisource production of final-state particles in high-energy nuclear collisions was proposed in several versions, which can be applied to study the transverse momentum distributions, elliptic flows, and so on. Final-state particles emit from different emission sources in the model, which can only identify the qualitative temperature parameters of emission sources. In recent years, Tsallis statistics is widely used in the investigation of particle distribution in high-energy collisions. In this paper, we combine Tsallis statistics with the multisource model. Moreover, the relaxation time approximation of the collision term in the Boltzmann transport equation is applied in the improved model. We study the transverse momentum spectra for different centrality classes in Pb–Pb collisions at $\sqrt{s_{NN}} = 5.02$ TeV and $\sqrt{s_{NN}} = 2.76$ TeV. The model results are in agreement with experimental data measured by ALICE and CMS collaborations. The values of parameters T, q, and t_{ft}/τ are obtained. On this basis, the nuclear modification factor R_{AA} is reproduced.

The temperature T increases with collision centrality and collision energy due to the excitation degree of the multiparticle system. For the same reason, t_{ft}/τ increases with the collision centrality and the collision energy. The non-equilibrium degree q

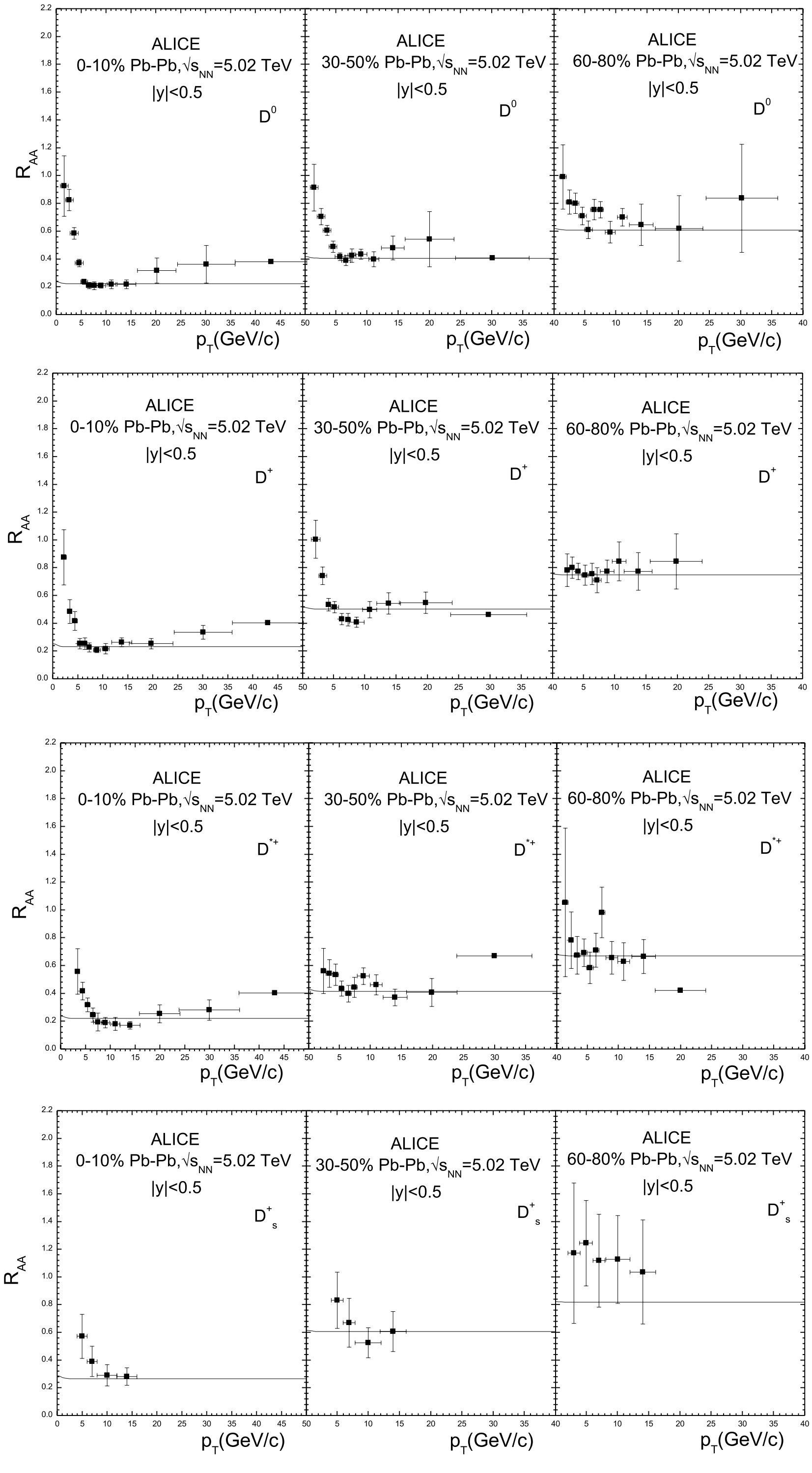

FIGURE 2
Nuclear modification factor R_{AA} of prompt D^0, D^+, D^{*+}, and D_s^+ mesons in the 0%–10%, 30%–50%, and 60%–80% centrality classes in Pb–Pb collisions at $\sqrt{s_{NN}}$ = 5.02 TeV. Symbols represent the experimental results obtained from ALICE collaboration [32]. The model results are represented by the curves.

at $\sqrt{s_{NN}}$ = 5.02 TeV is larger than that at $\sqrt{s_{NN}}$ = 2.76 TeV. The multiparticle system at the larger collision energy deviates farther from the equilibrium state. These thermodynamic properties may shed light on some information carried by particle distribution and are helpful in the better understanding of the particle production in high-energy collisions.

In the multisource thermal model, final-state particles emit from different emission sources, which are expected to be formed in

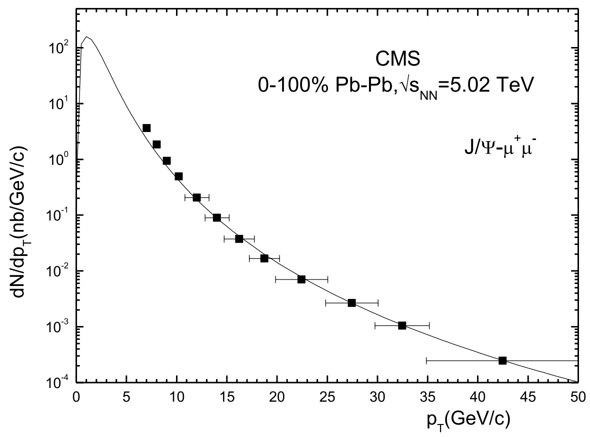

FIGURE 3
Differential cross section of the prompt J/Ψ meson decaying into two muons as a function of p_T in Pb−Pb collisions at $\sqrt{s_{NN}}$ = 5.02 TeV. Symbols represent the experimental results obtained from CMS collaboration [33]. The model results are represented by the curves.

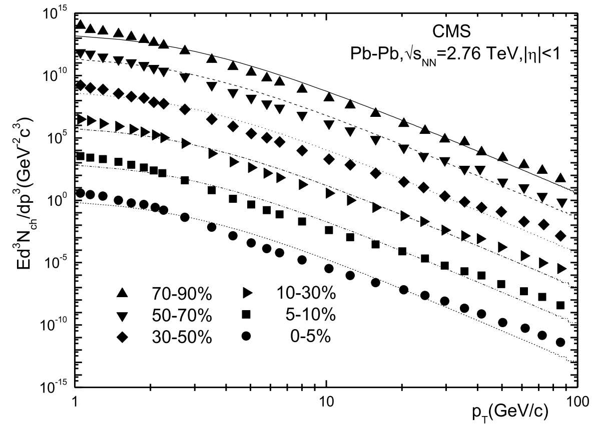

FIGURE 5
Transverse momentum distributions of charged particles in the 70%–90%, 50%–70%, 30%–50%, 10%–30%, 5%–10%, and 0%–5% centrality classes in Pb−Pb collisions at $\sqrt{s_{NN}}$ = 2.76 TeV. Symbols represent the experimental results obtained from CMS collaboration [34]. The model results are represented by the curves.

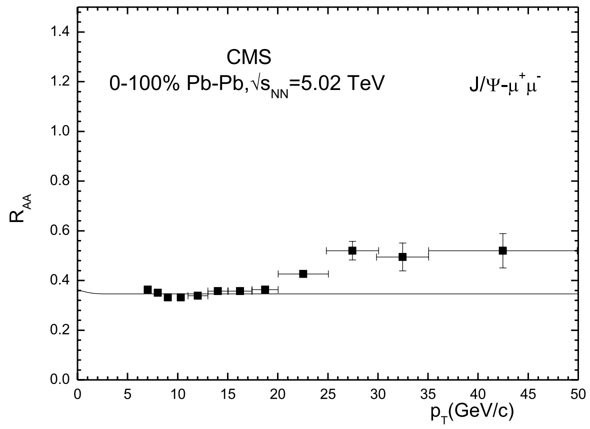

FIGURE 4
Nuclear modification factor R_{AA} of the prompt J/Ψ meson as a function of p_T in the Pb−Pb collisions at $\sqrt{s_{NN}}$ = 5.02 TeV. Similar to Figure 3, the experimental data are represented by the symbols, and the model results are represented by the curves. Experimental data are obtained from the CMS collaboration [33].

collisions. The model is still in development. The present work will further be improved in the framework of multisource production. The interaction of emission sources is related to the hot dense matter in the sources and also results in the azimuthally anisotropic expansion in the momentum space. The momentum asymmetry will be used to describe the elliptic flows of particles produced in ultra-relativistic heavy-ion collisions. Considering different rapidity shifts of anisotropic emission sources, the particle distribution in the rapidity space can be discussed. In the future, more properties of the multiparticle system will be found in the model and some thermodynamic quantities (such as the heat capacity, speed of sound, and conformal symmetry breaking measure) can be calculated.

Altogether, this work is a new attempt to study the properties of particle distribution using the improved method.

TABLE 2 Fitted values of q, T, and t_{ft}/τ shown in Figure 5.

Centrality	q	T	t_{ft}/τ	χ^2/NDF
0%–5%	1.114	0.150	0.905	1.485
5%–10%	1.115	0.148	0.875	1.430
10%–30%	1.115	0.145	0.805	1.405
30%–50%	1.114	0.143	0.715	1.383
50%–70%	1.115	0.139	0.665	1.388
70%–90%	1.115	0.137	0.562	1.392

Data availability statement

The original contributions presented in the study are included in the article/Supplementary Material; further inquiries can be directed to the corresponding author.

Author contributions

Y-FG: formal analysis, investigation, and writing–original draft. B-CL: methodology, project administration, writing–original draft, and writing–review and editing.

Funding

The authors declare that the financial support was received for the research, authorship, and/or publication of this article. This work was supported by the National Natural Science Foundation of China under Grant Nos 12147215, 12047571, and 11575103, the Shanxi Provincial Natural Science Foundation under Grant No. 202103021224036, the Scientific and Technological Innovation Programs of Higher Education Institutions in Shanxi (STIP) under Grant No. 201802017, and the Fund for Shanxi "1331 Project" Key Subjects Construction

Conflict of interest

The authors declare that the research was conducted in the absence of any commercial or financial relationships that could be construed as a potential conflict of interest.

Publisher's note

All claims expressed in this article are solely those of the authors and do not necessarily represent those of their affiliated organizations, or those of the publisher, the editors, and the reviewers. Any product that may be evaluated in this article, or claim that may be made by its manufacturer, is not guaranteed or endorsed by the publisher.

References

1. Adams J, Adler C, Aggarwal MM, Ahammed Z, Amonett J, Anderson BD, et al. Transverse momentum and collision energy dependence of high p_T hadron suppression in Au+Au collisions at ultrarelativistic energies. *Phys Rev Lett* (2003) 91:172302. doi:10.1103/PhysRevLett.91.172302

2. Adam J, Adamczyk L, Adams JR, Adkins JK, Agakishiev G, Aggarwal MM, et al. Strange hadron production in Au+Au collisions at sNN = 7.7, 11.5, 19.6, 27, and 39 GeV. *Phys Rev C* (2020) 102:034909. doi:10.1103/PhysRevC.102.034909

3. Abelev B, Adam J, Adamova D, Adare AM, Aggarwal MM, Rinella GA, et al. Pion, kaon, and proton production in central Pb-Pb collisions at sNN =2.76 TeV. *Phys Rev Lett* (2012) 109:252301. doi:10.1103/PhysRevLett.109.252301

4. Acharya S, Adamova D, Adler A, Adolfsson J, Aggarwal MM, Rinella GA, et al. Centrality and transverse momentum dependence of inclusive J/ψ production at midrapidity in Pb-Pb collisions at sNN =5.02 TeV. *Phys Lett B* (2020) 805:135434. doi:10.1016/j.physletb.2020.135434

5. Cleymans J, Worku D. The Tsallis distribution in proton–proton collisions at s = 0.9 TeV at the LHC. *J Phys G* (2012) 39:025006. doi:10.1088/0954-3899/39/2/025006

6. Tripathy S, Bhattacharyya T, Garg P, Kumar P, Sahoo R, Cleymans J. Nuclear modification factor using Tsallis non-extensive statistics. *The European Physical Journal A* (2016) 52:289. doi:10.1140/epja/i2016-16289-4

7. Braun-Munzinger P, Magestro D, Redlich K, Stachel J. Hadron production in Au - Au collisions at RHIC. *Phys Lett B* (2001) 518:41–6. doi:10.1016/s0370-2693(01)01069-3

8. Wolschin G. Beyond the thermal model in relativistic heavy-ion collisions. *Phys Rev C* (2016) 94:024911. doi:10.1103/physrevc.94.024911

9. Rafelski J, Letessier J. Testing limits of statistical hadronization. *Nucl Phys A* (2003) 715:98–107c. doi:10.1016/s0375-9474(02)01418-5

10. Kapusta JI. Perspective on Tsallis statistics for nuclear and particle physics. *Int J Mod Phys E* (2021) 30:2130006. doi:10.1142/s021830132130006x

11. Srivastava PK, Singh A, Chaturvedi OSK, Raina PK, Singh BK. Transverse momentum distribution of charged hadrons based on wounded quark model. *Eur Phys J A* (2019) 55:69. doi:10.1140/epja/i2019-12741-3

12. Gupta R, Jena S. Model comparison of the transverse momentum spectra of charged hadrons produced in PbPb collision at sNN =5.02 TeV. *Adv High Energ Phys.* (2022) 2022:5482034. doi:10.1155/2022/5482034

13. Liu FH, Abd Allah NN, Singh BK. Dependence of black fragment azimuthal and projected angular distributions on polar angle in silicon-emulsion collisions at 4.5A-GeV/C. *Phys Rev C* (2004) 69:057601. doi:10.1103/physrevc.69.057601

14. Shao GC, Li HL. Rayleigh-like distribution of particle transverse momenta in collisions at high energies. *Chin Phys. C* (2004) 34:964. doi:10.1088/1674-1137/34/7/007

15. He XW, Wu FM, Wei HR, Hong BH. Energy dependent chemical potentials of light hadrons and quarks based on transverse momentum spectra and yield ratios of negative to positive particles. *Adv High Energ Phys.* (2020) 2020:1–19. doi:10.1155/2020/1265090

16. Tsallis C. Possible generalization of Boltzmann-Gibbs statistics. *J Stat Phys* (1988) 52:479–87. doi:10.1007/bf01016429

17. Bediaga I, Curado EMF, de Miranda JM. A Nonextensive thermodynamical equilibrium approach in e+ e- ---> hadrons. *Physica A* (2000) 286:156–63. doi:10.1016/s0378-4371(00)00368-x

18. Abelev BI, Adams J, Aggarwal MM, Ahammed Z, Amonett J, Anderson BD, et al. Strange particle production in p+p collisions sNN = 200 GeV. *Phys Rev C* (2007) 75(064901). doi:10.1103/PhysRevC.75.064901

19. Adare A, Afanasiev S, Aidala C, Ajitanand NN, Akiba Y, AlBataineh H, et al. Measurement of neutral mesons in p+p collisions at sNN = 200 GeV and scaling properties of hadron production. *Phys Rev D* (2011) 83:052004. doi:10.1103/PhysRevD.83.052004

20. Aamodt K, Abel N, Abeysekara U, Quintana AA, Abramyan A, Adamova D, et al. Transverse momentum spectra of charged particles in proton-proton collisions at s =900 GeV with ALICE at the LHC. *Phys Lett B* (2010) 693:53. doi:10.1016/j.physletb.2010.08.026

21. Aamodt K, Abel N, Abeysekara U, Abrahantes Quintana A, Abramyan A, Adamová D, et al. Production of pions, kaons and protons in pp collisions at s =900 GeV with ALICE at the LHC. *Eur Phys J C* (2011) 71:1655. doi:10.1140/epjc/s10052-011-1655-9

22. ALICE Collaboration. Measurement of (anti) nuclei production in p-Pb collisions at sNN = 8.16 TeV (2022). Available at: https://arxiv.org/abs/2212.04777.

23. Acharya S, Adamova D, Adhya SP, Adler A, Adolfsson J, Aggarwal MM, et al. Measurement of Λ (1520) production in pp collisions at s = 7 TeV and p-Pb collisions at sNN = 5.02 TeV. *Eur Phys J C* (2020) 80:160. doi:10.1140/epjc/s10052-020-7687-2

24. Abelev BB, Adam J, Adamová D, Aggarwal MM, Agnello M, Agostinelli A, et al. Neutral pion production at midrapidity in pp and Pb-Pb collisions at sNN = 2.76 TeV. *Eur Phys J C* (2014) 74:3108. doi:10.1140/epjc/s10052-014-3108-8

25. Tasevsky M. [ALICE, ATLAS, CMS, LHCb, LHCf and TOTEM], Soft QCD measurements at LHC (2018). Available at: https://arxiv.org/abs/1802.02818.

26. Aad G, Abbott B, Abdallah J, Abdelalim AA, Abdesselam A, Abdinov O, et al. Charged-particle multiplicities in*pp*interactions measured with the ATLAS detector at the LHC. *New J Phys* (2011) 13:053033. doi:10.1088/1367-2630/13/5/053033

27. Chatrchyan S, Khachatryan V, Sirunyan AM, Tumasyan A, Adam W, Bergauer T, et al. Study of the Production of Charged Pions, Kaons, and Protons in pPb Collisions at sNN = 5.02 TeV. *Eur Phys J C* (2014) 74:2847. doi:10.1140/epjc/s10052-014-2847-x

28. Khachatryan V, Sirunyan AM, Tumasyan A, Adam W, Bergauer T, Dragicevic M, et al. [CMS]. Transverse momentum and pseudorapidity distributions of charged hadrons in pp collisions at s =0.9 and 2.36 TeV. *JHEP* (2010) 02:041. doi:10.1007/JHEP02(2010)041

29. Li BC, Fu YY, Wang LL, Wang EQ, Liu FH. Transverse momentum distributions of strange hadrons produced in nucleus-nucleus collisions at sNN = 62.4 GeV and 200 GeV. *J Phys G* (2012) 39:025009. doi:10.1088/0954-3899/39/2/025009

30. Li BC, Fu YY, Wang LL, Liu FH. Dependence of elliptic flows on transverse momentum and number of participants in Au + Au collisions at sNN = 200 GeV. *J Phys G* (2013) 40:025104. doi:10.1088/0954-3899/40/2/025104

31. Deppman A, Megias E, Menezes DP. Fractals, nonextensive statistics, and QCD. *Phys Rev D* (2020) 101:034019. doi:10.1103/physrevd.101.034019

32. Deppman A, Megias E, Menezes DP. Fractal structures of yang–mills Fields and non-extensive statistics: Applications to high energy physics. *MDPI Phys* (2020) 2: 455–80. doi:10.3390/physics2030026

33. Cleymans J, Worku D. Relativistic thermodynamics: Transverse momentum distributions in high-energy physics. *Eur Phys J A* (2012) 48:160. doi:10.1140/epja/i2012-12160-0

34. Acharya S, Acosta FT, Adamova D, Adolfsson J, Aggarwal MM, Rinella GA, et al. Measurement of D0D+, D*+ and Ds+ production in Pb-Pb collisions at sNN =5.02 TeV. *JHEP* (2018) 10:174. doi:10.1007/JHEP10(2018)174

35. Sirunyan AM, Tumasyan A, Adam W, Ambrogi F, Asilar E, Bergauer T, et al. Measurement of prompt and nonprompt charmonium suppression in PbPb collisions at 5.02 TeV. *Eur Phys J C* (2018) 78:509. doi:10.1140/epjc/s10052-018-5950-6

36. Chatrchyan S, Khachatryan V, Sirunyan AM, Tumasyan A, Adam W, Bergauer T, et al. Study of high-pT charged particle suppression in PbPb compared to pp collisions at sNN =2.76 TeV. *Eur Phys J C* (2012) 72:1945. doi:10.1140/epjc/s10052-012-1945-x

37. Abelev B, Adam J, Adamova D, Adare AM, Aggarwal MM, Aglieri Rinella G, et al. [ALICE]. Centrality dependence of π, K, p production in Pb-Pb collisions sNN = 2.76 TeV. *Phys Rev C* (2013) 88:044910. doi:10.1103/PhysRevC.88.044910